

# Topological Massive Dirac Edge Modes and Long-Range Superconducting Hamiltonians

O. Viyuela<sup>1</sup>, D. Vodola<sup>2</sup>, G. Pupillo<sup>2</sup> and M.A. Martin-Delgado<sup>1</sup>

1. Departamento de Física Teórica I, Universidad Complutense, 28040 Madrid, Spain.

2. icFRC, IPCMS (UMR 7504) and ISIS (UMR 7006),  
Université de Strasbourg and CNRS, 67000 Strasbourg, France.

We discover novel topological effects in the one-dimensional Kitaev chain modified by long-range Hamiltonian deformations in the hopping and pairing terms. This class of models display symmetry-protected topological order measured by the Berry phase of the ground state and the winding number of the Hamiltonians. For exponentially-decaying hopping amplitudes, the topological sector can be significantly augmented as the penetration length increases, something experimentally achievable. For power-law decaying superconducting pairings, the massless Majorana modes at the edges get paired together into a massive non-local Dirac fermion localised at both edges of the chain: a new topological quasiparticle that we call *topological massive Dirac fermion*. This topological phase has fractional topological numbers as a consequence of the long-range couplings. Possible applications to current experimental setups and topological quantum computation are also discussed.

PACS numbers: 74.20.Mn, 03.65.Vf, 71.10.Pm, 67.85.-d

1. *Introduction.*— The quest for the experimental realisation of topological superconductors has turned out to be far more elusive than for their insulating counterparts. Simple models for topological superconductors have been proposed [1, 2], but yet their unambiguous implementation is challenging in condensed matter or with quantum simulations. Here we address the issue as to whether those simple models [3, 4] are in fact very specific in hosting their long sought-after topological properties. Quite on the contrary, we find that these properties can not only be generic with respect to natural extensions of the model-Hamiltonian terms, but also that Hamiltonian deformations can give rise to unconventional topological edge-mode physics that is novel per se and for applications in topological quantum computation.

The appearance of topological superconductors has revolutionised condensed matter physics and quantum simulators. A tremendous effort is now directed at the experimental demonstration of existing topological models and at the development of new ones that may be easier to realise. What makes a topological superconductor interesting is the presence of Majorana modes as zero-energy localized modes at the edges or boundaries of the material. These modes lie within the superconducting gap and are rather exotic since Majorana fermions are their own anti-particles (holes). Standard (non-topological) superconductors do not exhibit such modes in their energy spectrum. Thus, topological superconductors represent new physics: Majorana modes are topologically protected against local perturbations disturbing the system and cannot be removed unless a topological phase transition occurs. This robustness makes them useful for storing and manipulating quantum information in a topological quantum computer.

In this paper we focus on the Kitaev chain model and propose novel modifications of the basic Hamiltonian, in

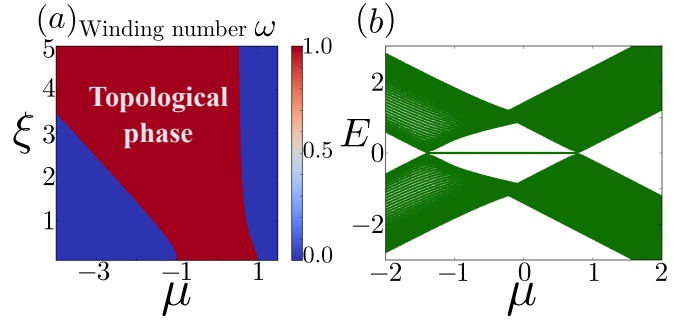


FIG. 1: (a) Topological phase diagram for the Kitaev chain with exponentially decaying hopping. As the penetration length  $\xi$  increases, the topological phase ( $\Phi_B = \pi\omega = \pi$ ) gets enlarged. For  $\xi \rightarrow 0$  we recover the well-known Majorana chain with nearest-neighbour hopping only. (b) Energy spectrum for  $\xi = 0.8$ . The region with Majorana zero modes  $\mu \in (-1, 1)$  in the original model has been augmented in one to one correspondence with a non-trivial Berry phase and winding number.

order to enrich the appearance of Majorana physics (see Fig. 1) and even new topological excitations (see Fig. 2, Fig. 3). These modifications come in two ways: a) exponentially decaying kinetic terms [see Eq. (6)] and b) long-range (LR) interaction terms [see Eq. (8)]. They produce novel beneficial topological effects and new unconventional topological physics, respectively. In case a), we propose a hopping deformation that allows us to significantly increase the region in the phase diagram where Majorana modes are present. Interestingly enough, this modification may result in a realistic description for cold atoms in optical lattices. In case b), we study the topological properties of another complementary modification of the Kitaev model based on long-range pairing terms decaying algebraically with a certain exponent  $\alpha$  [see Eq. (8)]. We discover novel topological effects not found

in any simple model before (see Fig. 2): for  $\alpha < 1$  the model suffers a major qualitative change manifested in the absence of Majorana modes that are transmuted onto Dirac modes, which are massive non-local edge states. The topological protection of these new edge states is guaranteed by their non-local extension, they neither break the odd fermion parity condition nor other discrete symmetries like particle-hole, etc. and they appear as mid-gap superconducting states that can not be absorbed into bulk states. These topological massive Dirac edge states are new physical quasiparticles that are absent in the standard Kitaev model. They represent a new unconventional topological phase.

**2. Long-range deformations of superconducting Hamiltonians.**— We consider a model of spinless fermions on a  $L$ -site one-dimensional chain, with  $p$ -wave superconducting pairing and a hopping term. The Hamiltonian of the system is

$$H = \sum_{j=1}^L \left( -J \sum_{l=1}^{L-1} \frac{1}{r_{l,\xi}} a_j^\dagger a_{j+l} + M \sum_{l=1}^{L-1} \frac{1}{d_{l,\alpha}} a_j a_{j+l} - \frac{\mu}{2} (a_j^\dagger a_j - \frac{1}{2}) + \text{h.c.} \right), \quad (1)$$

where  $\mu$  is the chemical potential,  $J > 0$  is the hopping amplitude, the absolute value of  $M = |M|e^{i\Theta}$  stands for the superconducting gap,  $a_j$  ( $a_j^\dagger$ ) are annihilation (creation) fermionic operators. The Hamiltonian deformations are  $r_{l,\xi}$ ,  $d_{l,\alpha}$ . They are generic functions of an integer distance  $l$ , and parameters  $\xi$  and  $\alpha$ , respectively [see Eqs. (6) and (8)]. The total number of fermions modulo 2 is called the 'fermion parity' and it is a conserved quantity for all models in (1). Considering only nearest-neighbours hopping and pairing, we recover the famous model introduced by Kitaev [4]. This model is topological displaying Majorana zero modes (MZM) at the edges like in Fig. 2(a). In the topological phase, the ground state of the Kitaev model is two-fold degenerate: bulk eigenstates have even parity due to the paired condensate, while the two Majorana modes at the edges amount to a single ordinary fermion of odd parity. The conservation of fermion parity and the non-local character of the unpaired Majoranas at the edges make the system an ideal candidate for a topological qubit out of the two-fold degenerate ground state [5, 6].

Without loss of generality, we may fix the pairing amplitude to be real and  $M = J = 1$ . Assuming periodic boundary conditions, we can diagonalize the Hamiltonian deformations (1) in Fourier space and in the Nambu-spinor basis representing paired fermions [7]:  $H = \sum_k \Psi_k^\dagger H_k \Psi_k$ , where  $\Psi_k = (a_k, a_{-k}^\dagger)^\dagger$  and  $H_k$  is of the form  $H_k = \Delta_k \mathbf{n}_k \cdot \boldsymbol{\sigma}/2$ . The gap of the system is given by  $\Delta_k$ ,  $\boldsymbol{\sigma}$  is the Pauli matrix vector and  $\mathbf{n}_k$  is a

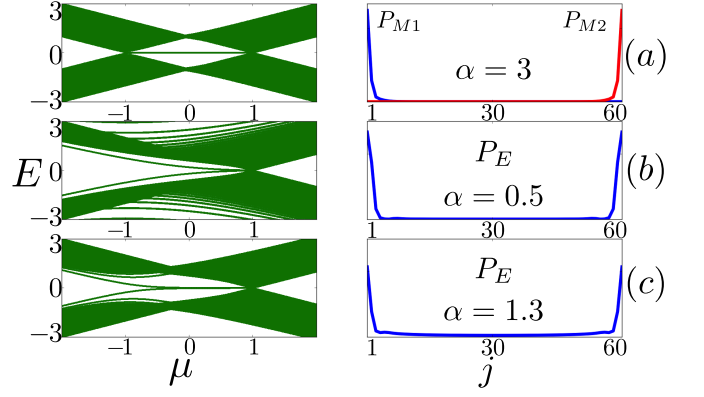


FIG. 2: Left side, we plot the spectrum for the Kitaev chain with long-range decaying pairing (see (8)), for  $L = 60$  sites. On the right hand side we show the probability distribution  $P_E$  of the edge modes for different topological phases. (a) Majorana phase with  $\alpha = 3$ . We can see MZM for  $\mu \in [-1, 1]$  localised at the edges of the chain, as plotted on the right hand side for  $\mu = -0.5$  ( $P_{M1}$  and  $P_{M2}$ ). Notice that each Majorana mode is decoupled, represented with different colors. (b) Massive Dirac phase with  $\alpha = 0.5$ . Within the new topological phase ( $\mu < 1$ ), there are topological massive Dirac fermions localised at both edges at the same time, as shown on the right hand side for  $\mu = -1.5$ . (c) Crossover phase with  $\alpha = 1.3$ . There are both Majorana zero modes and massive Dirac fermions depending on the value of  $\mu$ . We plot the probability for a massive Dirac fermion at  $\mu = -0.8$ .

unit vector called *winding vector*. Explicitly,

$$\mathbf{n}_k = -\frac{2}{\Delta_k} \left( 0, f_\alpha(k), \mu + g_\beta(k) \right), \quad \Delta_k = 2\sqrt{(\mu + g_\xi(k))^2 + f_\alpha^2(k)}, \quad (2)$$

with

$$g_\xi(k) = \sum_{l=1}^{L-1} \frac{\cos(k \cdot l)}{r_{l,\xi}} \quad \text{and} \quad f_\alpha(k) = \sum_{l=1}^{L-1} \frac{\sin(k \cdot l)}{d_{l,\alpha}}. \quad (3)$$

Particular instances of the functions  $r_{l,\xi}$  and  $d_{l,\alpha}$  have been considered in [8, 9], where long-range deformations of the Kitaev chain were first considered.

These models (2) still belong to the D symmetry class of topological insulators and superconductors [10, 11], with particle-hole symmetry and fermion parity preserved. These symmetries impose a restriction on the movement of the winding vector  $\mathbf{n}_k$  from the sphere  $S^2$  to the circle  $S^1$  on the  $yz$ -plane. Thus, we have a mapping from the reduced Hamiltonians  $H_k$  on the Brillouin zone  $k \in S^1$  onto the winding vectors  $\mathbf{n}_k \in S^1$ . This mapping  $S^1 \rightarrow S^1$  is characterized by a winding number  $\omega$ , a topological invariant defined as the angle swept by  $\mathbf{n}_k$  when the crystalline momentum  $k$  is varied across the whole Brillouin Zone (BZ) from  $-\pi$  to  $+\pi$ ,

$$\omega := \frac{1}{2\pi} \oint d\theta = \frac{1}{2\pi} \oint \left( \frac{\partial_k n_k^z}{n_k^y} \right) dk, \quad (4)$$

where we have used that  $\theta := \arctan(n_k^z/n_k^y)$ .

As a complementary tool in 1D systems, we can use the Berry/Zak phase [12–14] to characterize topological order. When the system is adiabatically transported from a certain crystalline momentum  $k_0$  up to  $k_0 + G$ , where  $G$  is a reciprocal lattice vector, the eigenstate of the lower band of the system  $|u_k^-\rangle$  picks up a topological Berry phase given by

$$\Phi_B = \oint A_B(k) dk. \quad (5)$$

The Berry connection  $A_B(k) = i\langle u_k^- | \partial_k u_k^- \rangle$  parallelly connects two infinitesimally close points on the many-fold defined by  $|u_k^-\rangle$  in  $k$  space. For the standard Kitaev chain [4], the resulting gauge-invariant phase  $\Phi_B$  is quantized (0 or  $\pi$ ) due to the particle-hole symmetry that characterises distinct topological phases in one to one correspondence with the winding number [15].

*3. Augmented topological phases induced by exponentially decaying hoppings.*— This remarkable effect is obtained choosing nearest-neighbour pairing, i.e.,  $d_{1,\alpha} = 1$  and  $d_{l>1,\alpha} = \infty$  and

$$r_{l,\xi} = \begin{cases} e^{\frac{(l-1)}{\xi}} & \text{if } l < L/2 \\ e^{\frac{L-1-l}{\xi}} & \text{if } l > L/2 \end{cases}, \quad (6)$$

where  $\xi$  is the penetration length of the exponentially decaying hopping terms. This Hamiltonian may be realisable in simulations of topological superconductors using cold atoms in optical lattices [16–18], where the exponential decay of the hopping terms with distance can be tuned, e.g., by varying the depth of the lattice potentials [19].

In Fig. 1 we plot the complete phase diagram by computing the winding number and the topological Berry phase from Eqs. (4) and (5). For  $\xi \rightarrow 0$  we recover the usual Kitaev chain. The system is topological for  $\mu \in [-1, 1]$ , displaying MZM at the edges. Interestingly enough, when we increase the penetration length  $\xi$ , the region where we observe MZM is augmented. In fact, this widening effect is purely due to the hopping deformation since we find that including an exponentially-decaying pairing deformation does not change the topological phases. The phase separation between the trivial and non-trivial topological phases can be computed analytically from Eq.(2), obtaining

$$\mu_{c1} = \frac{e^{\frac{1}{\xi}}}{1 + e^{\frac{1}{\xi}}}, \quad \mu_{c2} = \frac{e^{\frac{1}{\xi}}}{1 - e^{\frac{1}{\xi}}}. \quad (7)$$

Thus, increasing the penetration length of the deformed hopping, we can arbitrarily enlarge the topologically non-trivial sector (see Fig. 1). Although symmetry-protected topological order is usually associated with local interactions, we have shown that non-local terms can favour the formation of a topological phase. Qualitatively similar

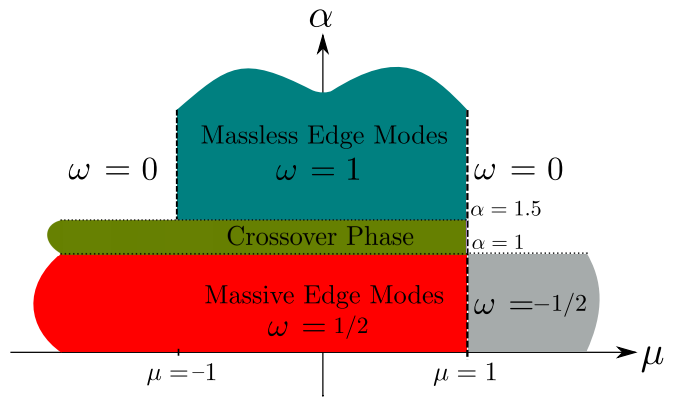


FIG. 3: Topological phase diagram for the Kitaev chain with long-range pairing (8). The wavy lines at the border of certain phases indicate that they extend endlessly. Fractional topological numbers highlight the appearance of an unconventional topological phase with massive non-local Dirac edge states. The topological characterisation of the crossover phase is discussed in the main text and the Appendix.

effects have been recently observed in Ref. [20] for the spin-1 long-range Haldane model [21].

*4. Unconventional topological superconductivity with Dirac topological massive states*— Long-range deformations may not only enlarge topological phases but also produce new types of topological phases. To this end, let us now consider pairing terms that decay algebraically with a power-law exponent  $\alpha$ , and no deformation of the hopping terms. That is,  $r_{1,\xi} = 1$ ,  $r_{l>1,\xi} = \infty$  and

$$d_{\alpha,l} = \begin{cases} l^\alpha & \text{if } l < L/2 \\ (L-l)^\alpha & \text{if } l > L/2 \end{cases}. \quad (8)$$

In the thermodynamic limit  $L \rightarrow \infty$ , the function  $f_\alpha(k)$  in Eq. (3) is divergent at  $k = 0$  for  $\alpha < 1$ . This function defines the long-range pairing and appears in the energy gap and the winding vector of Eq. (2). Thus, the gap and the group velocity also become divergent at  $k = 0$  if  $\alpha < 1$ . Nevertheless,  $\omega$  [Eq. (4)] and  $\Phi_B$  [Eq. (5)] are still integrable. Moreover, it is not possible to gauge away the divergence from  $k = 0$  by means of a gauge transformation, as in the ordinary Kitaev chain. Therefore, the singularity behaves as a *topological defect*. A detailed discussion of this effect at  $k = 0$  on the topological indicators is carried out in Sec. I of the Appendix. According to the behaviour of  $f_\alpha(k)$  at  $k = 0$ , we find 3 different topological phases depending on the exponent  $\alpha$ :

i/ Majorana Phase [ $\alpha > 3/2$ ]*—* this phase is topologically equivalent to the one of the short-range Kitaev chain [4]: For  $|\mu| > 1$ , the phase is topologically trivial and we do not find MZM. In the region  $\mu \in (-1, 1)$ , we find that MZM are always present [see Fig. 2(a)]. The function  $f_\alpha(k)$  is not divergent and we can compute the winding number  $\omega$  of Eq. (4) and the Berry phase  $\Phi_B$  of Eq. (5) obtaining  $\Phi_B = \pi\omega = \pi$ . The lower band eigen-

vector  $|u_k^- \rangle$ , thus, shows a  $U(1)$  phase discontinuity at  $k = 0$ . This topological region is depicted in blue in the phase diagram of Fig. 3.

ii/ Massive Dirac Phase [ $\alpha < 1$ ] $\text{---}$  an unconventional topological phase appears for sufficiently slow decaying pairing. As an example, in Fig. 2(b) we see for  $\alpha = 1/2$  two clearly different phases as a function of  $\mu$ . For  $\mu > 1$  the system is in a trivial phase, with no edge states. However, for  $\mu < 1$  the system has a topological massive Dirac fermion at the edges, as shown in the wave function plot in Fig. 2(b). The two Majorana modes at the two distant edges have paired up onto a single massive Dirac fermion. Notice that the fermion is highly non-local and its nature is deeply rooted in the long-range/non-local character of the pairing term. This topological quasi-particle is still protected by fermion parity: the ground state has still even parity, whereas the first excited state populates this non-local massive fermion and has odd parity. One cannot induce a transition between these two states without violating the fermion parity conservation of the Hamiltonian, and applying a non-local operation is needed. Moreover, the subspace of these two edge states is still protected by the bulk gap from the bulk excitations. In Sec. II of the Appendix, by finite-size scaling analysis we show that the mass of the Dirac fermion stays finite in the thermodynamic limit for  $\mu < 1$  and all  $\alpha < 1$ . This way we can prove that the effect is purely topological and caused by the long-range deformation.

When we close the chain, the edge states disappear as we may expect for a topological effect. Despite the long-range pairing coupling, the system still belongs to the D symmetry class [10, 11], since no discrete symmetry has been broken. The winding number  $\omega$  can still be formally defined using Eq. (4). However, the topological defect at  $k = 0$  deeply modifies the value of  $\omega$ . For the trivial phase  $\mu > 1$ , the winding number is  $\omega = -1/2$ , whereas for the new unconventional topological phase is  $\omega = +1/2$  if  $\mu < 1$ . The semi-integer character of  $\omega$  is associated to the integrable divergence at  $k = 0$ , which modifies the continuous mapping  $S^1 \rightarrow S^1$ . Notwithstanding, in this region there is still a jump of one unit between the two topologically different phases,  $\Delta\omega = \omega_{\text{top}} - \omega_{\text{trivial}} = 1$  (see Fig. 3). Moreover, the topological indicators take on the same value within the whole phase until the bulk gap closes at  $\mu = 1$ , giving rise to a topological phase transition, and the new massive topological edge states disappear. Therefore, we can still establish a bulk-edge correspondence. There is a novelty in this case regarding the parallel transport for the Berry phase.

Namely, at  $k = 0$  the adiabatic condition breaks down since both the energy gap and the quasi-particle group velocity diverge. Moreover, the singularity at  $k = 0$  of the lower band eigenvector  $|u_k^- \rangle$ , cannot be removed by a simple gauge transformation as it is not just a  $U(1)$

phase difference, but a phase shift unitary jump,

$$|u_{k \rightarrow 0+}^- \rangle = e^{i\pi P_{\pm}} |u_{k \rightarrow 0-}^- \rangle, \quad (9)$$

where  $P_{\pm} = \frac{1}{2}(\mathbb{1} \pm \sigma_z)$ . More explicitly,

$$e^{i\pi P_-} = \begin{pmatrix} 1 & 0 \\ 0 & e^{i\pi} \end{pmatrix}, \quad e^{i\pi P_+} = \begin{pmatrix} e^{i\pi} & 0 \\ 0 & 1 \end{pmatrix}. \quad (10)$$

The difference in sign  $\pm$  of the projector  $P_{\pm}$  depends on the topological sector. For  $\mu > 1$ , the system is in a trivial phase with no edge states and the long-range singularity of  $|u_k^- \rangle$  at  $k = 0$  is given by  $e^{i\pi P_-}$ . On the other hand for  $\mu < 1$ , the system is in a topological phase with massive and non-local edge states. The singularity of  $|u_k^- \rangle$  at  $k = 0$  in that case is given by  $e^{i\pi P_+}$ .

iii/ Crossover Phase [ $\alpha \in (1, 3/2)$ ] $\text{---}$  this is a crossover region between phases i/ and ii/. There are massless Majorana edge states for  $1 > \mu > \mu_c$  like in phase i/, but for  $\mu < \mu_c$  the edge states become massive as in phase ii/. The critical value of  $\mu_c$  depends on  $\alpha$  and it approaches  $\mu_c = -1$  when  $\alpha \rightarrow 3/2$ . Within this phase, the quasi-particle group velocity still diverges but the energy gap does not, and the structure of the topological defect at  $k = 0$  changes accordingly. The winding number is not able to capture the whole “mixed” character of this phase. However, as detailed in the in Sec. I of the Appendix, we can clearly see that the behaviour of the winding vector and the lower-band eigenstate is different from the other two phases. In Fig. 3, we present a complete phase diagram summarising the different topological and trivial phases of the model as a function of  $\mu$  and  $\alpha$ .

5. *New form of topological quantum computation.* $\text{---}$  In the massive Dirac topological phase ( $\alpha < 1$ ), the ground state is unique and has even fermion parity. The first excited state corresponds to populating the massive Dirac fermion at the edges and has odd fermion parity. As shown in Fig. 2(b), this effective two level system is separated from the bulk eigenstates by an energy gap. The conservation of fermion parity and the non-local character of the massive Dirac fermion, makes the system an ideal candidate for a topological qubit out of this gapped two-fold subspace. The topological protection is usually associated to a degenerate subspace. Outstandingly, we have found a gapped two level system that is however topologically protected from the bulk excitations. A concrete proposal for topological quantum computation with non-local massive Dirac fermions is feasible in the spirit of [22].

6. *Outlook and Conclusions.* We have found that finite-range and long-range extensions of the one-dimensional Kitaev chain can be used as a resource for enhancing existing topological properties and for unveiling new topological effects. In particular, for long-range pairing deformations, we observe non-local massive Dirac

fermions characterised by fractional topological numbers. Hamiltonians with long-range pairing and hopping may be realised in Shiba chains as recently proposed in [23, 24], where edge states can be detected, e.g., by scanning tunneling spectroscopy [25]. Alternatively, next-nearest neighbour hopping may be harnessed in atomic and molecular setups [17], where massive edge modes should be observable via a combination of spectroscopic techniques and single-site addressing [26, 27]. The extension of existing models for gapped topological qubits may boost the search for long-range deformations in more complicated topological models with symmetry-protected or even intrinsic topological order.

M.A.MD. and O.V. thank the Spanish MINECO grant FIS2012-33152, the CAM research consortium QUITEMAD+ S2013/ICE-2801, the U.S. Army Research Office through grant W911NF-14-1-0103, FPU MEC Grant and Residencia de Estudiantes. G.P and D.V. acknowledge support by the ERC-St Grant ColdSIM (No. 307688), EOARD, UdS via Labex NIE and IdEX, RYSQ.

- 
- [1] M. Z. Hasan and C. L. Kane, *Rev. Mod. Phys.* **82**, 3045 (2010).
  - [2] X.-L. Qi and S.-C. Zhang, *Rev. Mod. Phys.* **83**, 1057 (2011).
  - [3] N. Read, D. Green, *Phys. Rev. B* **61**, 10267 (2000).
  - [4] A. Y. Kitaev, *Phys.-Usp.* **44**, 131 (2001).
  - [5] Chetan Nayak, Steven H. Simon, Ady Stern, Michael Freedman, and Sankar Das Sarma, *Rev. Mod. Phys.* **80**, 1083 (2010).
  - [6] B. M. Terhal, *Rev. Mod. Phys.* **87**, 307 (2015).
  - [7] A. Altland and B. Simons, *Condensed Matter Field Theory* (Cambridge University Press, New York, 2010).
  - [8] D. Vodola, L. Lepori, E. Ercolessi, A. V. Gorshkov, G. Pupillo, *Phys. Rev. Lett.* **113**, 156402 (2014).
  - [9] D. Vodola, L. Lepori, E. Ercolessi, G. Pupillo, *arXiv*: 1508.00820 (2015).
  - [10] A. P. Schnyder, S. Ryu, A. Furusaki and A. W. W. Ludwig, *Phys. Rev. B* **78**, 195125 (2008).
  - [11] A. Kitaev, *AIP Conf. Proc.* **1134**, 22 (2009).
  - [12] M. V. Berry, *Proc. R. Soc. A* **392**, 45 (1984).
  - [13] B. Simon, *Phys. Rev. Lett.* **51**, 2167 (1983).
  - [14] J. Zak, *Phys. Rev. Lett.* **62**, 2747 (1989).
  - [15] O. Viyuela, A. Rivas and M. A. Martin-Delgado, *Phys. Rev. Lett* **112**, 130401 (2014).
  - [16] P. Massignan, A. Sanpera, and M. Lewenstein, *Phys. Rev. A* **112**, 031607 (2010).
  - [17] L. Jiang, T. Kitagawa, J. Alicea, A. R. Akhmerov, D. Pekker, G. Refael, J. I. Cirac, E. Demler, M. D. Lukin, and P. Zoller, *Phys. Rev. Lett* **106**, 220402 (2011).
  - [18] A. Bühler, N. Lang, C.V. Kraus, G. Möller, S.D. Huber and H.P. Büchler, *Nat. Comm.* **5**, 4504 (2014).
  - [19] I. Bloch, J. Dalibard, and W. Zwerger, *Rev. Mod. Phys.* **80**, 885 (2008).
  - [20] Z.-X. Gong, M. F. Maghrebi, A. Hu, M. Foss-Feig, P. Richerme, C. Monroe, A. V. Gorshkov, *arXiv*: 1510.02108 (2015)
  - [21] Z.-X. Gong, M. F. Maghrebi, A. Hu, M. L. Wall, M. Foss-Feig, A. V. Gorshkov, *arXiv*: 1505.03146 (2015).
  - [22] S. B. Bravyi, A. Y. Kitaev, *Annals of Physics*, **298**, 1 210-226 (2002).
  - [23] F. Pientka, L.I. Glazman and F. von Oppen, *Phys. Rev. B* **88** 155420 (2013).
  - [24] F. Pientka, L.I. Glazman and F. von Oppen, *Phys. Rev. B* **89** 180505(R) (2014).
  - [25] A. Yazdani, B. A. Jones, C. P. Lutz, M. F. Crommie, and D. M. Eigler, *Science* **275**, 1767 (1997).
  - [26] W. S. Bakr, J. I. Gillen, A. Peng, S. Fölling, and M. Greiner, *Nature* **462**, 74 (2009).
  - [27] J. F. Sherson, C. Weitenberg, M. Endres, M. Cheneau, I. Bloch and S. Kuhr, *Nature* **467**, 68 (2010).



## APPENDIX

### I. Winding vector and Berry phase in the presence of a Topological Defect

In the thermodynamic limit  $L \rightarrow \infty$ , the function  $f_\alpha(k)$  in (3) tends to

$$f_\alpha(k) = \frac{i}{2} \left( \text{Li}_\alpha(e^{-ik}) - \text{Li}_\alpha(e^{ik}) \right). \quad (\text{A1})$$

where  $\text{Li}_\alpha(e^{ik})$  is a polylogarithmic function. This function defines the long-range pairing and is divergent at  $k = 0$  for  $\alpha < 1$ . As a consequence, the energy gap in (2) diverges if  $\alpha < 1$ , and the particle group velocity  $v_g = \partial_k \Delta_k$  diverges for  $\alpha < 3/2$  at  $k = 0$ . In line with this, we can trace the effect of this divergence over the winding vector and the topological phases within the different topological sectors:

i/ Majorana Phase [ $\alpha > 3/2$ ]— There is no topological defect in this phase. The winding number and the Berry phase can be computed using (4) and (5). We find the same topological indicators and the same type of edge states physics as for the short range Kitaev model ( $\alpha \rightarrow \infty$ ). In Fig. A1 we plot the winding vector for  $L = 201$  sites and for different values of the chemical potential  $\mu$  belonging to different topological regimes. We can see that for trivial regions  $|\mu| > 1$ , the winding vector winds back and forth and never covers the entire  $S^1$  circle. On the other hand, when the system is within a topological phase  $\mu \in (-1, 1)$ , the winding vector winds around  $S^1$  completely. The lower band eigenvector  $|u_k^- \rangle$  can always be chosen to be periodic. If the system is in the trivial phase,  $|u_k^- \rangle$  is also continuous, whereas in the topological phase, there is a  $U(1)$  phase discontinuity at  $k = 0$ , i.e.,

$$|u_{k \rightarrow 0^+}^- \rangle = e^{i\pi} |u_{k \rightarrow 0^-}^- \rangle. \quad (\text{A2})$$

This phase shift can be gauged away from  $k = 0$ , and it represents the Berry phase gained by the system after an adiabatic transport from a certain crystalline momentum  $k_0$  up to  $k_0 + G$ , where  $G$  is a reciprocal lattice vector.

ii/ Massive Dirac Phase [ $\alpha < 1$ ]— The topological defect at  $k = 0$  makes the winding vector ill-defined at that point, although its contribution to the winding number can still be integrated. In Fig. A2 we plot the winding vector for  $L = 301$  sites and for different values of  $\mu$ . In particular, for  $\mu > 1$  the winding vector covers the entire lower half of the  $S^1$  circle, explaining the value  $\omega = -1/2$  of the winding number. On the contrary, for  $\mu < 1$ , the winding vector just covers the entire upper half of  $S^1$  as shown in the figure. The function  $f_\alpha(k)$  at  $k = 0$  diverges as

$$f_\alpha(k \rightarrow 0^-) \rightarrow -\infty, \quad f_\alpha(k \rightarrow 0^+) \rightarrow \infty. \quad (\text{A3})$$

Hence, in the transition from  $k < 0$  to  $k > 0$ , the winding vector skips the entire lower part of the  $S^1$  circle

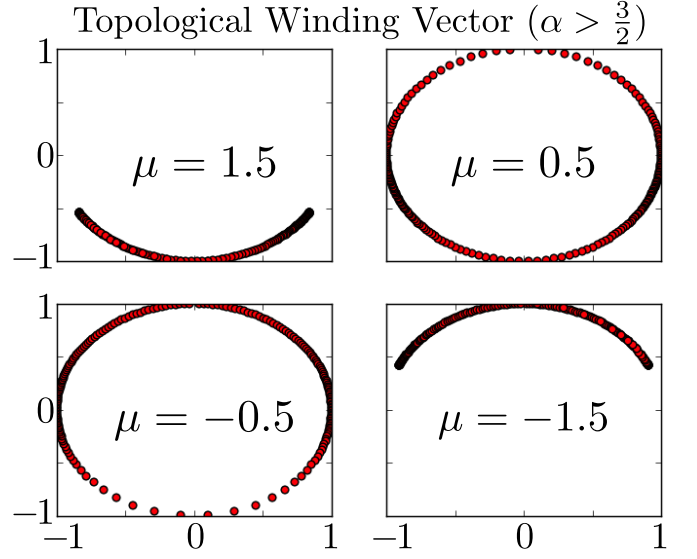


FIG. A1: Trajectories of the winding vector for different sectors within the Majorana phase, for  $L = 201$  sites and  $\alpha = 3$ . The red spots represent the movement of the winding vector along the unit circle  $S^1$ . As we see, for  $\mu > 1$  and  $\mu < -1$ , the vector never winds around the whole  $S^1$ , just moving back and forth twice. However, if  $\mu \in (-1, 1)$  the vector winds around  $S^1$ . The darker regions highlight a larger density of points.

because of the topological defect at  $k = 0$ . This explains the value of the winding vector  $\omega = +1/2$  in this new topological phase. Complementary, the adiabatic condition breaks down at  $k = 0$  as the quasi-particle group velocity diverges. Therefore, we can no longer say that the system picks up a  $U(1)$  phase after a close loop in momentum space. Actually, the singularity at  $k = 0$  of the lower band eigenvector  $|u_k^- \rangle$ , cannot be removed by a simple gauge transformation as it is not just a  $U(1)$  phase difference, but a phase shift unitary jump,

$$|u_{k \rightarrow 0^+}^- \rangle = e^{i\pi P_\pm} |u_{k \rightarrow 0^-}^- \rangle, \quad (\text{A4})$$

where  $P_\pm = \frac{1}{2}(\mathbb{1} \pm \sigma_z)$ . More explicitly,

$$e^{i\pi P_-} = \begin{pmatrix} 1 & 0 \\ 0 & e^{i\pi} \end{pmatrix}, \quad e^{i\pi P_+} = \begin{pmatrix} e^{i\pi} & 0 \\ 0 & 1 \end{pmatrix}. \quad (\text{A5})$$

The difference in sign  $\pm$  of the projector  $P_\pm$  depends on the topological sector. For  $\mu > 1$ , the system is in a trivial phase with no edge states and the singularity of the eigenstate at  $k = 0$  is given by  $e^{i\pi P_-}$ . On the other hand for  $\mu < 1$ , the system is in a topological phase with massive and non-local edge states. The singularity of the eigenstate at  $k = 0$  in that case is given by  $e^{i\pi P_+}$ .

iii/ Crossover Phase [ $\alpha \in (1, 3/2)$ ]— This is a crossover region between the previous two phases i/ and ii/. In this case, the structure of the topological defect at  $k = 0$  has changed. The components of the winding vector are continuous, but their derivatives diverge. Therefore, the

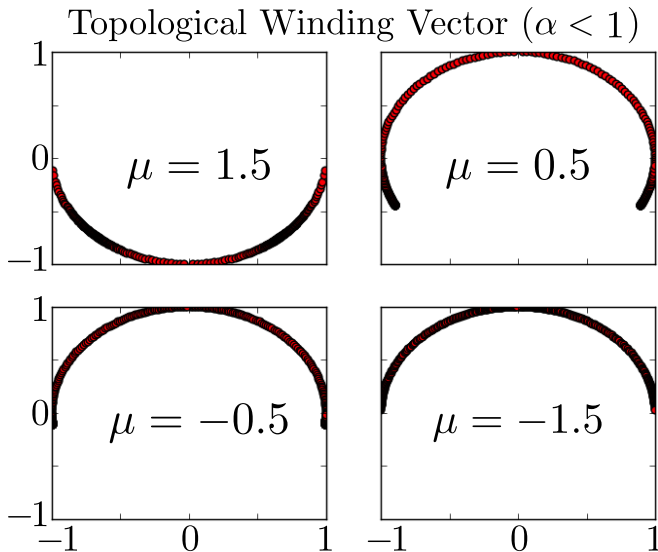


FIG. A2: Trajectories of the winding vector for different sectors within the massive Dirac phase, for  $L = 301$  sites and  $\alpha = 0.5$ . The red spots represent the movement of the winding vector along the unit circle  $S^1$ . For  $\mu > 1$ , the winding vector covers the lower half of  $S^1$ . However, if  $\mu < 1$  the vector covers only the upper half of the circle. The darker regions highlight a larger density of points.

population of points close to  $k = 0$  is extremely dispersive. The winding vector does not cover the entire south pole sector due to the divergence in the derivatives of its components in the thermodynamic limit. Hence, the behaviour of the winding vector is different than in the other two previous phases A and B. This might be linked to the mixed character of the phase with the presence of Majorana zero modes and massive Dirac fermions depending on the concrete value of  $\mu$  and  $\alpha$ . Regarding the lower band eigenvector, it is continuous but its derivative is still divergent at  $k = 0$  breaking the adiabatic condition.

## II. Edge mass gap finite-size scaling

In Sec. IV of the main text, we claimed that the pairing of the Majorana zero modes into a massive non-local Dirac fermion cannot be explained as a simple interaction between the Majorana fermions at the edges due to a finite size effect. Actually, its nature is deeply rooted to the long-range/non-local character of the pairing deformation of the Kitaev chain. The absence of a degenerate zero energy subspace avoids a wave function superposition to localise a single Majorana mode at one edge only. On the contrary, the two edges are inevitably coupled to each other, pairing to a non-local massive Dirac mode as shown in Fig. 2.

In order to proof this claim more rigorously, we have computed the mass of the edge states through a finite-

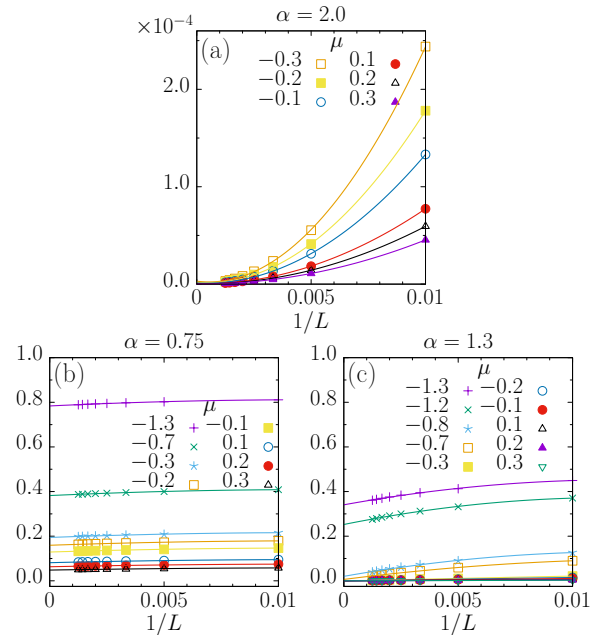


FIG. A3: Finite size scaling of the edge mass gap for different values of the exponent  $\alpha$  and the chemical potential  $\mu$ . In (a) we plot the case for  $\alpha = 2.0$  belonging to the Majorana phase. The edge mass gap closes with  $L$  for every  $\mu$  within the topological phase. In (b) we take  $\alpha = 0.75$  in the massive Dirac phase. For  $\mu < 1$  the edge mass gap tends to a finite value in the thermodynamic limit. In (c) we perform the finite-size scaling for  $\alpha = 1.3$  in the crossover phase. We have both massless and massive edge states depending on the value of  $\mu$ .

size scaling for different values of the decaying exponent  $\alpha$  and the chemical potential  $\mu$  (see also Ref.[9]).

In Fig. A3(a) we perform a finite-size scaling for the masses of the Majorana zero modes for the Majorana phase. Within the topological sector  $\mu \in (-1, 1)$ , the edge mass gap clearly goes to zero with  $L$  as we expected. On the other hand, in Fig. A3(b) we perform the same finite-size scaling analysis for the massive Dirac phase. In this case, there are edge states for  $\mu < 1$ . As we can see, the masses of the edge states go to a finite value even in the thermodynamic limit. This proves that the topological nature of the non-local massive Dirac fermions purely comes from the long-range deformation of the original Kitaev Hamiltonian and not from a finite size effect. Finally, Fig. A3(c) shows the finite-size scaling for the edge mass gap within the crossover phase. Although there are edge states all over  $\mu < 1$ , we can clearly see a finite region  $\mu \in (1, \mu_c)$  where the edge states are massless, whereas for  $\mu < \mu_c$  the edge states become massive. This phase displays a mixed character between the Majorana and the massive Dirac phases. The critical value of  $\mu_c$  depends on  $\alpha$  and it approaches  $\mu_c = -1$  when  $\alpha \rightarrow 3/2$ .